Extended Data figures

Fig S1. Characterization of BCMA/PD-L1/PD-L2 in bone marrow and extramedullary disease of R/R MM.

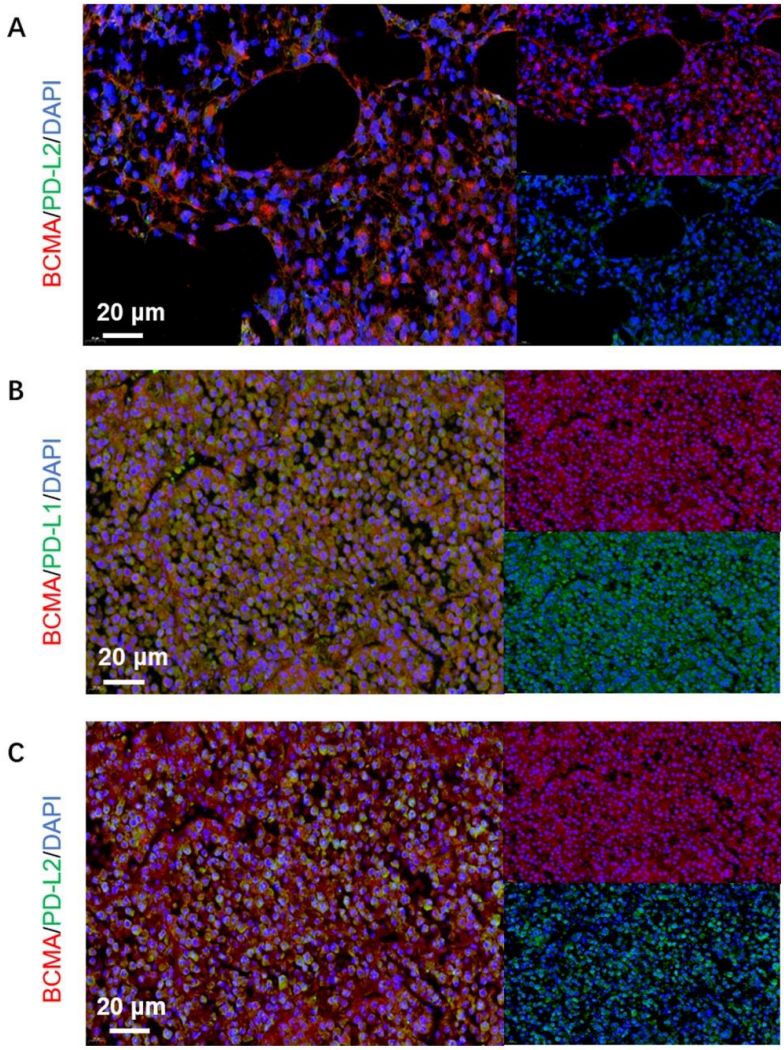

A. Representative immunofluorescence staining pictures showing the expression of PD-L2 and their colocalization in BM sample from R/R MM patient. Scale bar, 20 mm.
B. Representative immunofluorescence staining pictures showing the expression of PD-L1 and their colocalization in extramedullary disease sample from R/R MM patient. Scale bar, 20 mm.
C. Representative immunofluorescence staining pictures showing the expression of PD-L2 and

their colocalization in extramedullary disease sample from R/R MM patient. Scale bar, 20 mm.

Fig S2. PD-L1 overexpression results in decreased cytotoxicity and cytokine secretion

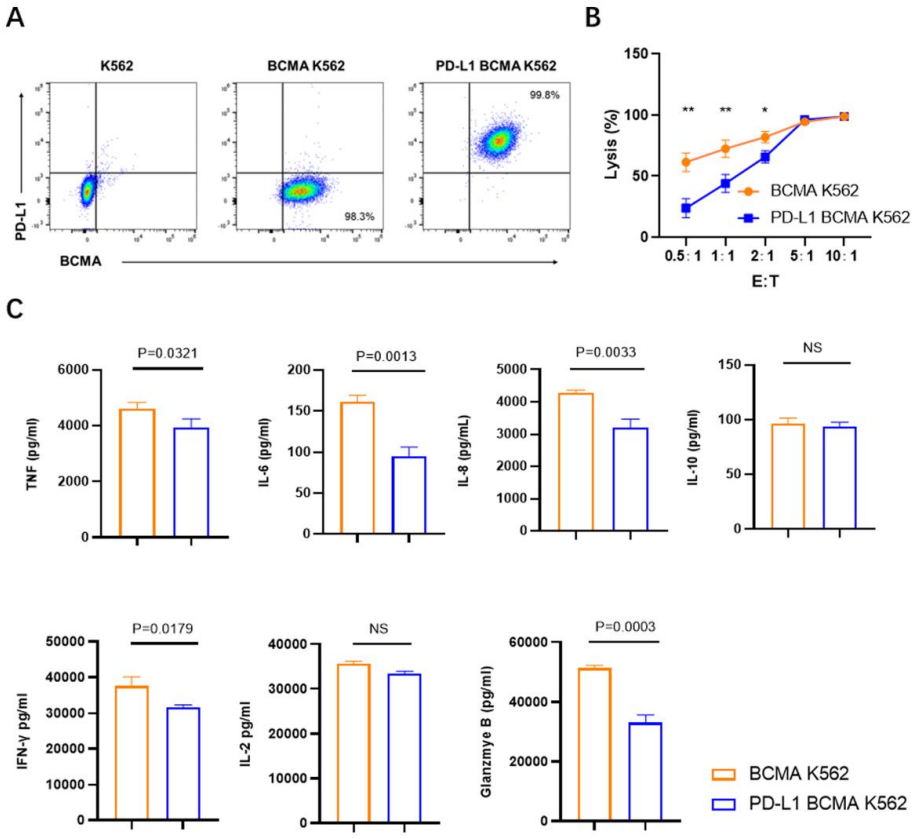

A. Identification of BCMA over-expressed K562 cells and PD-L1/BCMA over-expressed K562 cells by flow cytometry.

B. In vitro cytotoxicity of BCMA targeting CAR-T cells against BCMA over-expressed K562 cells and PD-L1/BCMA over-expressed K562 cells was determined by luciferase-based cytotoxicity assay. E/T ratio, effector/target ratio. Data are shown as the mean ± s.e.m. (n=3 independent healthy donors). Statistical significance was determined by Mantel-Cox test, presented by $^{**}P < 0.01$, $^{*}P < 0.05$.

C. Cytokine secretion measured by luminex technology in the supernatant after co-culture with PD-L1/BCMA over-expressed K562 cells for 24 h. Data are shown as the mean ± s.e.m.

(n = 3 independent healthy donors). IL-2, interleukin-2; IL-6, interleukin-6; IL-8, interleukin-8; TNFα, tumor necrosis factor α; IFNγ, interferon-γ

Fig S3. Construction and Validation of an shRNA-Specific Predictive Algorithm

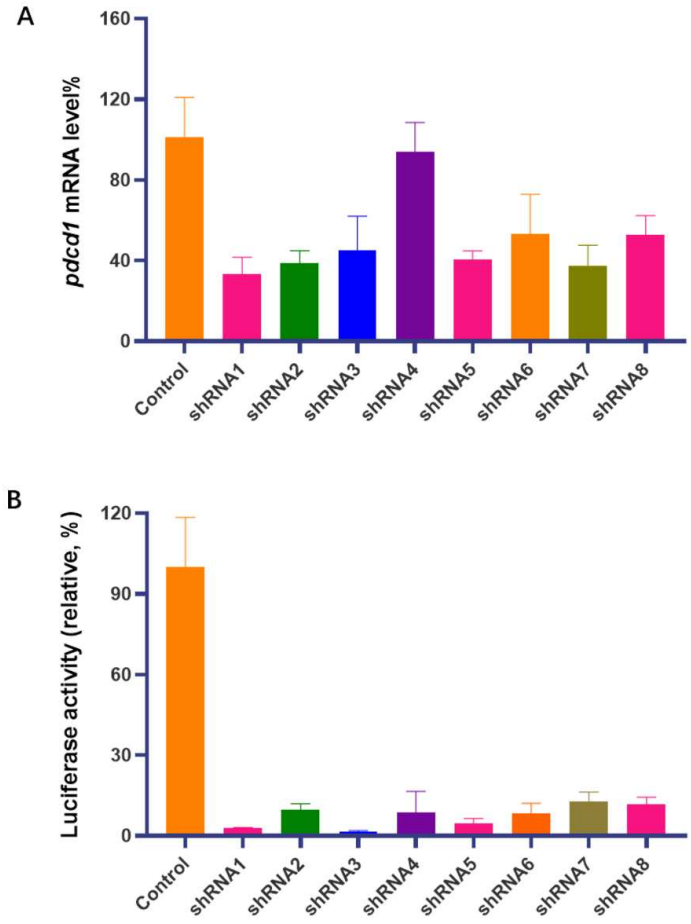

A. Knockdown efficiencies for shRNAs targeting the human gene *PDCD1* within the retroviral vector which contains *PDCD1*, luciferase gene and anti-PD-1 shRNA scaffold. Expression of *PDCD1* in 293T cells was tested by qPCR.

B. Knockdown efficiencies for shRNAs targeting the human gene firefly luciferase gene within the retroviral vector which contains *PDCD1*, luciferase gene and anti-PD-1 shRNA scaffold. Expression of luciferase in 293T cells was tested by Dual-Luciferase Reporter Assay.

Fig S4. Anti-tumor efficacy was verified in anti-CLL-1 and anti-CD19 CAR-T cells with or without anti-PD-1 shRNA construct.

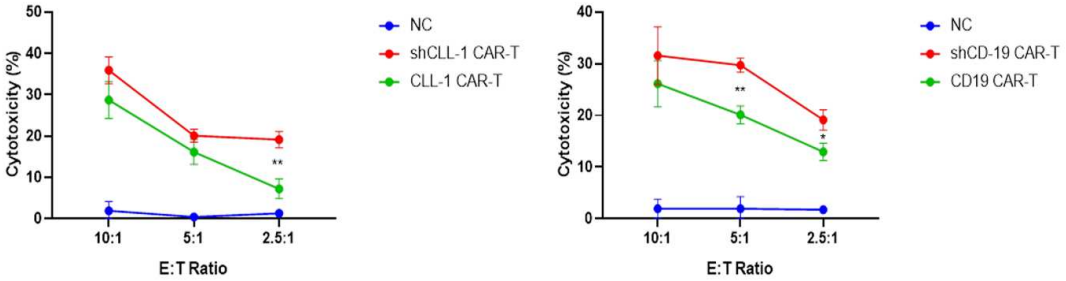

In vitro cytotoxicity of CLL-1 targeting CAR-T cells against PD-L1/CLL-1 over expressed U937 cells or CD19 targeting CAR-T cells against PD-L1 over expressed Raji cells was determined by LDH-based cytotoxicity assay. E/T ratio, effector/target ratio. Data are shown as the mean ± s.e.m. (n=3 independent healthy donors). Statistical significance was determined by Mantel-Cox test, presented by $^{**}P < 0.01$, $^{*}P < 0.05$.

Fig S5. The principal component analysis for bulk RNA-seq data

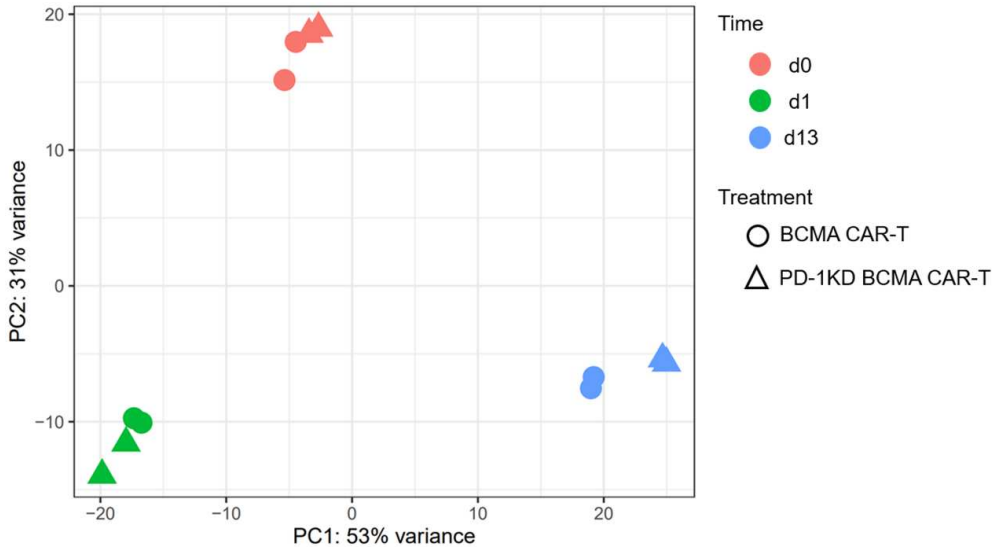

The PCA was utilized to elucidate the variation in the bulk RNA transcriptomes. The transcripts of BCMA targeting CAR-T cells with and without PD-1 shRNA in a separate time overlapped, whereas the transcripts in different timepoints make distinct clusters. Data shown are from two independent healthy donors.

Fig S6. Clinical response after CAR-T infusion.

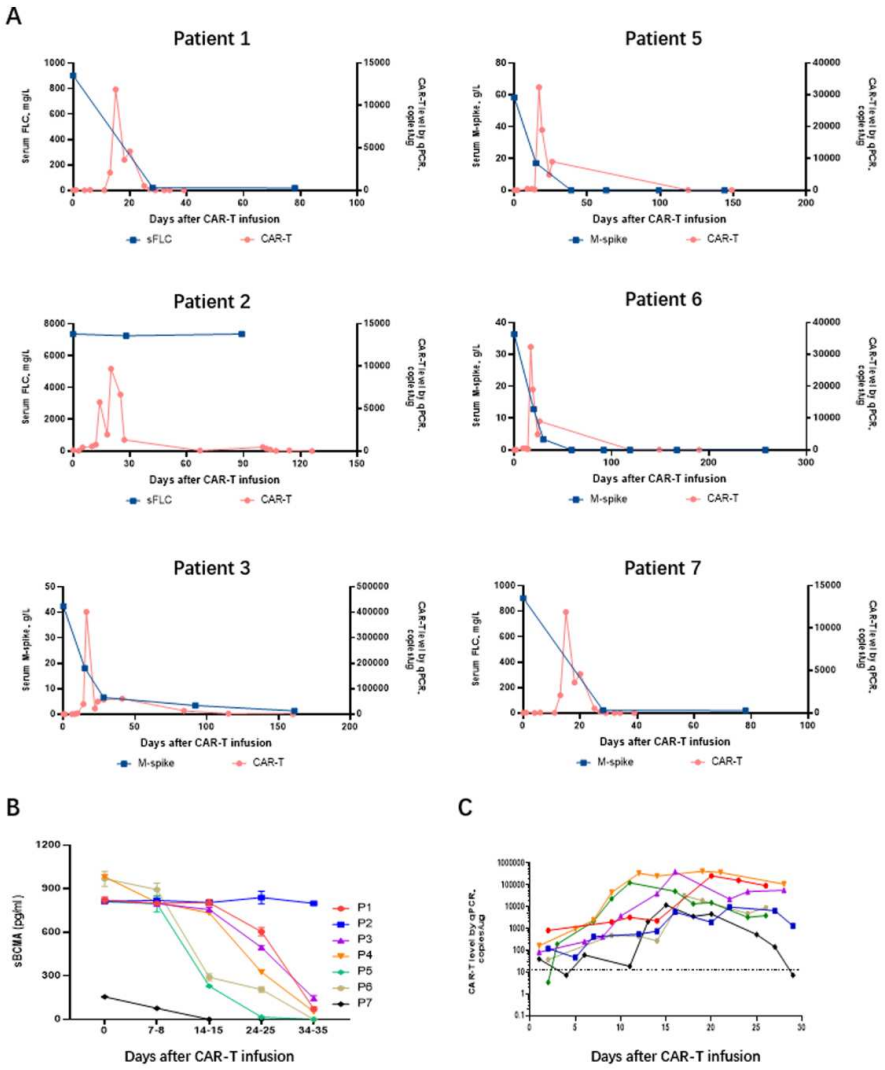

A. All patients except patient 2 exhibited a marked decline in serum M-spike or serum free light chain (blue) after CAR-T cell infusion coincident with a rise in numbers of circulating CAR-T cells (pink). sFLC, serum free light chain.

B. Dynamics of sBCMA concentrations in the plasma determined by ELISA assay.

C. Peripheral blood levels of CART-BCMA in the first 30 days after infusion determined by

qPCR for vector sequences

Fig S7. In vitro and in vivo evaluation of PD-1^{KD} BCMA CAR-T cells products.

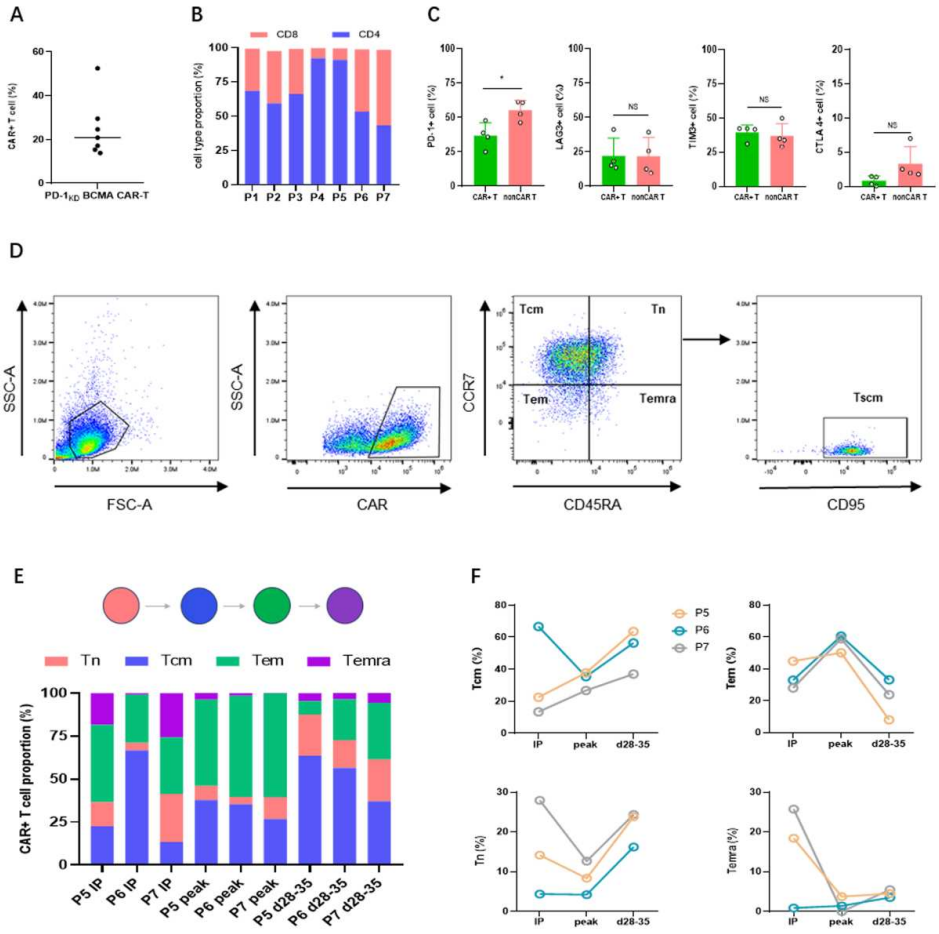

A. Percentage of CAR+ cells in the final products of the seven RR MM patients.

B. CD4+ and CD8+ cell proportion in the final products of the seven RR MM patients.

C. Comparison of PD1/LAG3/TIM3/CTLA4 expression in CAR+ and CAR- cells detected by flow cytometry without antigen stimulation in four representative infusion products. *P < 0.05.

D. Gating scheme used for the identification of CAR+ T cell subtypes.

E. Immunophenotypic characterization of three highly responsive patients with either CR or

sCR in the product and after infusion. IP, infused product.

F. Longitudinal contribution of each subpopulation to the CAR cell compartment in the three highly responsive patients.